https://doi.org/10.1016/j.apr.2021.101169

Characteristics of particle emissions from light duty diesel vehicle fueled with ultralow sulphur diesel and biodiesel blend

Bei Wang[1*], Wing-Hong Or[1], Shun-Cheng Lee[2], Yiu-Cheong Leung[3], Bruce Organ[4], Kin-Fai Ho[5*]

[1] *Faculty of Science and Technology, Technological and Higher Education Institute of Hong Kong, Hong Kong*

[2] *Department of Civil and Environmental Engineering, The Hong Kong Polytechnic University, Hong Kong*

[3] *Department of Mechanical Engineering, The University of Hong Kong, Hong Kong*

[4] *Jockey Club Heavy Vehicle Emissions Testing and Research Centre, Hong Kong*

[5] *Jockey Club School of Public Health and Primary Care, The Chinese University of Hong Kong, Sha Tin, Hong Kong*

***Corresponding authors:**

E-mail address: beiwang@thei.edu.hk (B. Wang), kfho@cuhk.edu.hk (K.-F. Ho).

Abstract

This study investigates the particle emissions from a diesel vehicle fueled with ultralow sulphur diesel (B0, ULSD) and 5% biodiesel blend (B5) by a chassis dynamometer test under three driving conditions. Elemental carbon (EC), organic carbon (OC), 30 species of polycyclic aromatic hydrocarbon (PAH) and 10 species of oxygenated PAH (oxy-PAH) were analyzed to quantify the chemical compositions of the collected particulate matter (PM). The emission factors (*EF*s) of OC were increased with B5 by a range between 39.5% and 113.7%, compared with B0. Both fuel blends recorded a trace amount of EC (0.25 mg/kg or less). It was found that the B5 *EF*s of total PAHs were decreased by a range between 15.2% and 50.2% relative to B0. 2- to 3-ring species, the dominant PAHs and oxy-PAHs, were decreased substantially when using B5. However, the results showed that biodiesel blend promoted the emission of 4- and 5-ring oxy-PAHs and 5- to 7-ring PAHs. The application of B5 shifted the composition towards a higher proportion of PAHs with higher molecular weight and more oxy-PAHs. Due to the increased emissions in PAHs with higher toxic equivalent factors (TEFs), the application of B5 resulted in an increase in toxicity expressed in BAP_{eq} range from 11.3% to 117.0%.

Keywords – PM, OC/EC, PAHs, Vehicle exhaust.

1. Introduction

Diesel vehicular emission, which is one of the major sources of ambient aerosols, could cause severe adverse health effects (USEPA, 2002). There were 131,000 licensed diesel commercial vehicles in Hong Kong in 2016 (equivalent to around 18% of the total vehicle number), and they accounted for over 90% of road-side $PM_{2.5}$ emissions (Panel on Environmental Affairs, Legislative Council of HKSAR, 2018). Biodiesel, which is an oxygenated diesel made from vegetable oils, animal fats, or waste cooking oil by the transesterification reaction, is considered as one of the sustainable alternatives to diesel fuel for transportation purpose. Biodiesel is widely used to refer to fatty acid esters, most common fatty acid methyl esters (FAME). One of the most important difference between biodiesel and fossil diesel is that biodiesel has higher oxygen content (Knothe and Razon, 2017), which could lead to the differences in exhaust emission when biodiesel or its blends are used as motor fuel.

Several studies reported lower emissions of particulate matter (PM) from biodiesel blends compared to diesel fuel (Bakeas et al., 2011a; Karavalakis et al., 2016; Lapuerta et al., 2008; Na et al., 2015). With the addition of biodiesel, the chemical composition of the emitted PM might be very different because of higher oxygen content and lower aromatic content in biodiesel. However, there are limited information on chemical compositions of the particle emission such as elemental carbon (EC), organic carbon (OC), particulate-phase polycyclic aromatic hydrocarbons (PAHs), and oxygenated polycyclic aromatic hydrocarbons (oxy-PAHs). Some studies reported that biodiesel would reduce EC emissions (Lapuerta et al., 2008; Lu et al., 2012; Tsai et al., 2010; Zhang et al., 2015). On the other hand, OC emissions were reported to increase slightly (Lu et al., 2012; Zhang et al., 2009; Zhang et al., 2015) or decrease (Zhang et al., 2009) due to the difference in the chemical composition, physical properties of the testing fuel and different experimental setups such as engine speed and loading. The heterogeneous effects of biodiesel on OC and EC may change the composition of total carbon (TC) emissions. Williams et al. (2012) reported that OC accounted for the higher proportion of TC when the biodiesel content increased, and concluded that particulate exhausts from biodiesel contained more OC. Similar impact was reported by Zhang et al. (2009) who compared B20 blend with diesel in different engine speed and loading combination, since the reduction of EC (over 30% in most cases) was always larger than OC. However, Agarwal et al. (2013) reported a reduced OC proportion in TC for particulate exhaust from B20 compared to that from diesel and attributed this to biodiesel having higher oxygen content, which could facilitate more efficient combustion and a relative reduced emission of unburnt hydrocarbon.

PM contains various toxic pollutants including PAHs. In 2012 IARC reclassified diesel engine exhausts as Group 1 (carcinogenic to humans) from Group 2A (probably carcinogenic to humans) (IARC, 2012). Previous studies reported that diesel vehicular emission is one of the most important PAHs emission sources (Chen et al., 2013; Shen et al., 2011). Incomplete combustion processes do not only emit PAHs but also oxy-PAHs. Moreover, oxy-PAHs may also be produced from photochemical reactions of PAHs (Walgraeve et al. 2015). Oxy-PAHs may pose a higher health concern than PAHs due to their potentially higher mutagenicity (Maria del Rosario Sienra, 2006; Tomaz et al., 2017). Several studies found that the effect of fuel type on emission levels and toxicity of PAHs and oxy-PAHs from vehicular emissions was significant (Abrantes et al., 2009; He et al., 2010). While some studies suggested the total PAHs emissions to be reduced with biodiesels made from different raw materials (He et al., 2010; Lu et al., 2012; Tsai et al., 2010), the effects of biodiesel from waste cooking oil were reported inconsistently. Zhang et al. (2019) observed a drop in PAHs emissions, while Karavalakis et al. (2011) and Bakeas et al. (2011a) who tested a used frying oil methyl ester in blends from 10 to 50% v/v, observed a rise in PAHs and oxy-PAHs level.

The main goal of this study is to investigate the particle emissions from a light duty diesel vehicle in three driving conditions with B0 and B5. The chemical composition of PM emitted from the tested vehicle including carbonaceous species (i.e. OC and EC), PAHs, and oxy-PAHs would be evaluated.

2. Methodology

2.1. Overview of tested vehicle, fuel, and instrumentation set-up

The tested vehicle was Hyundai H1, a Euro-VI light duty diesel vehicle. It was equipped with several aftertreatment devices including diesel oxidation catalyst (DOC), diesel particulate filter (DPF), exhaust gas recirculation (EGR), and lean NO_x trap (LNT). The specification of the Euro VI tested vehicle is listed in Table 1.

The vehicle was tested with two types of fuels (i.e., B0 and B5). B0 is the ultralow sulphur content diesel (ULSD) and B5 is 5% waste cooking oil (WCO) derived biodiesel blended with 95% ULSD by volume. The reason of B5 is used in this study is that almost all diesel engines are easily compatible with blends up to B5 and the usage of blends of biodiesel higher than B5 may void the vehicles' original factory warranty. Besides, B5 blend is the specification of motor vehicle biodiesel in Hong Kong with the amended Air Pollution Control (Motor Vehicle Fuel) Regulation (Cap. 311L), and HKSAR government departments have been encouraged by the Environmental Protection Department to use B5 to promote popularization of biodiesel usage in Hong Kong (The Government of the HKSAR, 2019).

The neat WCO derived biodiesel (B100) was manufactured by Dynamic Progress Int. Ltd. Waste derived biodiesel was the only available biodiesel in Hong Kong, and the Environmental Protection Department has a certificate program for the biodiesel on the market as well as a registration program for waste cooking oils processors. The physico-chemical properties of B0 and neat biodiesel are listed in Table 2. The FAME profile of the neat biodiesel is given in Table 3.

The Euro VI-LDV was tested on a Mustang chassis dynamometer (48" single roller). A loading of 50% was applied to simulate actual condition by rising the roller resistance. The tailpipe of the tested vehicle was connected to the dilution tunnel and constant volume sampler (CVS), in which the tailpipe emission was diluted by zero air. Figure 1 shows the schematic diagram of the vehicle emission testing.

2.2. Driving cycles

In total, three types of driving conditions, namely transient, steady-state, and idling were carried out for the vehicle testing. For each combination of fuel blend and driving condition, three trials were performed. New European Driving Cycle (NEDC) test was adopted representing the transient condition. It has been the type approval process for homologating light duty vehicles in Europe, simulating an actual dynamic situation in urban area in the first part (780 s) and extraurban area in the second part (400 s). The vehicle speed at steady-state test was set at 50 km/h since it is the speed limit for the majority of roads in urban areas of Hong Kong. In order to achieve this constant speed, the vehicle was accelerated for 30 s. For idling test, the tested vehicle was parked on the chassis dynamometer with engine on. The testing duration of steady-state and idling cycle was 20 minutes.

2.3. PM sample collection

During each driving test, PM was collected on a pre-baked 47 mm Whatman quartz filter and a 46.2 mm Whatman Teflon filter simultaneously using two parallel filter holders. The filters were conditioned for at least 24 with relative humidity of 45% and temperature of 22 °C before weighing by a microbalance with 0.001 mg readability (MC5, Sartorius, Germany). All filters were weighed at least two times before and after collection of PM samples. It is required that the difference of two consecutive weightings was less then 0.01% of the filter weight. During sample collection and analyses, laboratory blanks and operational blanks were collected with the field sample. All the PM results were corrected with the laboratory and operation blanks.

2.4. Chemical analyses

The analyses of OC, EC, PAHs, and oxy-PAHs were conducted from the PM samples collected on the quartz filters. A specially designed chopper cut each quartz filter exactly in half. The contents of OC and EC were determined by the IMPROVE thermal/optical reflectance method (DRI Model 2001 Thermal/ Optical Carbon Analyzer) as described by Chow et al. (2007). The fractions of OC (i.e., OC1, OC2, OC3, and OC4) were produced in a non-oxidizing atmosphere (Helium) and the fractions of EC (i.e., EC1, EC2, and EC3) were produced in an oxidizing atmosphere (Helium with 2% oxygen). Some OC may pyrolytically convert to EC as optical pyrolysis (OP) during the volatilization of OC. A helium-neon laser was used to track the difference in reflectance to correct the fraction. The DRICarb software analysis package was used for data recording and processing. In this manuscript, OC refers to OC1+OC2+OC3+OC4+OP; EC refers to EC1+EC2+EC3; Total carbon (TC) refers to OC+EC.

The PM samples on another half portion of each quartz filter were analyzed for PAHs and oxy-PAHs determinations. The samples were quantified by the thermal desorption-gas chromatography/mass spectrometer (TD-GC/MS) method as described by Ho et al. (2008). Briefly, half portion of each filter was spiked with equivalent amounts (i.e., 2.0 ng) of four internal standards. The four internal standards were chrysene (chr-d12) and phenanthrene (phe-d10) (98%, Sigma-Aldrich) for parent PAHs (pPAHs), anthraquinone-d8 and benzophenone-d10 (98%, J&K chemical Ltd.) for oxy-PAHs, respectively. The filter portion was air-dried, and inserted into pre-baked TD tubes for analysis. The injector port temperature was at set 50 °C before sample tube loading and then raised to 275 °C in a splitless mode. After the injector temperature reached the set point, the oven temperature program started. The MSD was operated at full scan mode from 50 to 550 amu under electron impact ionization at a voltage of 70 eV and an ion source temperature of 230 °C. Identification was achieved by characteristic ion and retention times of the chromatographic peaks with those of authentic standards. Table 4 and Table 5 list the species of PAHs and oxy-PAHs analyzed.

2.5. Calculation of *EF*

EFs of the vehicle emission testing could be expressed either in distance-based or fuel-based approach. While a distance-based *EF* is commonly employed, it is unable to calculate such *EF* of idling test since the idling cycle is conducted without running the vehicle. Therefore, the fuel-based *EF* was calculated in this study. The fuel consumption for a driving test could be estimated by a carbon mass balance model given by Equation (1), considering the high combustion efficiency of the diesel engine. Thus, CO_2 can be reasonably assumed to be the major combustion product and the contribution of other carbon containing species is negligible.

$$\frac{V_f \times \rho_f \times \omega_f}{MW_C} = \frac{M_{CO_2}}{MW_{CO_2}} \qquad (1)$$

where,

V_f is the volume of consumed fuel [L]

ρ_f is density of fuel (B0: 0.83; B5: 0.8325) [kg/L]

ω_f is mass fraction of carbon in fuel (B0:0.87; B5: 0.86)

MW_C is molecular mass of carbon [g/mol]

M_{CO_2} is background corrected mass of CO_2 in each driving trial [g]

MW_{CO_2} is molecular mass of CO_2 [g/mol]

The foundation of Equation (1) is 1 mole of carbon atom in fuel producing 1 mole of CO_2. The *EFs* of OC, EC, PAHs, and oxy-PAHs could be quantified by dividing the compound amount emitted in the testing by the consumed fuel amount.

To evaluate the toxicity of the particulate phase PAH emissions, the TEFs of 16 PAHs with reference to benzo[*a*]pyrene (BaP) were used to calculate BaP equivalent (BaP_{eq}) for each driving condition with the use of B0 and B5 fuels (Nisbet & LaGoy, 1992). The total BaP_{eq} fuel-based *EFs* were the sum of the products of individual PAHs *EFs* and their corresponding TEF values.

3. Results and discussion

3.1. OC and EC

Generally, this study observed low *EF*s of OC and EC from the exhaust particulate samples, suggesting that the DPF has a high effectiveness to remove particulate exhaust emissions. Shibata et al. (2019) measured the carbonaceous aerosols emission from an engine with DPF and oxidation catalyst, and reported a reduction of 99.7% EC and 91.8% OC for diesel fuel, and 99.5% EC and 87.8% OC for B10 rapeseed methyl ester biodiesel blend, respectively. In this study, it was found that the EC contents emitted from both B0 and B5 fuels were very close to the detection limit over all three driving cycles. They were even below the detection limit in several trials/samples. As a result, a very low EC *EF* and a very high OC to TC ratio was observed for each driving conditions as shown in Figure 2. Previous study also reported a particularly high proportion of OC for diesel vehicles equipped with a DPF (from 0.74 to 0.98), even for vehicles with a high odometer (Wang et al., 2015). The vehicle tested in this study meets the latest emission standard and has a very low odometer, the emissions of EC were lower, and the OC accounted for an even higher proportion of TC (above 0.95), compared to the study of Wang et al. (2021). Apart from the influence of a DPF, biodiesel may contribute to a high OC proportion due to the greater reduction in EC and the less reduction or even promotion in OC (Williams et al., 2012; Zhang et al., 2009). In this study, the OC to TC ratios of different fuel blends and driving cycles were within a close range, the proportion of OC accounted for 94.8% to 99.9% of the TC. The application of B5 increased the ratio by 1.4% over idling, but decreased it by 0.3% and 4.3% over NEDC and steady-state respectively.

Figure 2 shows the *EF*s of OC and EC in different driving conditions. The OC *EF*s of B0 across the driving cycles were between 2.86 ± 0.33 and 7.19 ± 1.51 mg/kg, and those of B5 were between 4.31 ± 0.64 and 15.36 ± 3.77 mg/kg. It was found that the average EC *EF*s for B0 ranged from 0.01 ± 0.00 to 0.11 ± 0.10 mg/kg, while the average EC *EF*s for B5 ranged from 0.02 ± 0.02 to 0.25 ± 0.39 mg/kg. Both B0 and B5 generated the highest OC *EFs* under idling and the lowest *EFs* at NEDC. Higher OC emissions during idling as compared to other driving conditions has been reported in previous paper for vehicles equipped with a DPF (Wang et al., 2021). Shah et al. (2004) found that the major particulate species during idle and slow driving were OC. During idling condition fuel consumption increased and engine temperature decreased, due to a fuel lean condition which excess air acts as a cooler, resulting in an incomplete fuel combustion and higher OC emission (Fraser et al., 2002). Under idling state, B5 raised OC *EF*s by 114% compared to B0. The rise in OC *EF*s was 50.6% in NEDC and 39.5% in steady-state cycle, respectively. It was found that EC *EFs* varied significantly across driving cycles (i.e., from - 80% to + 816%) by the use of

B5. As the EC content detected for each trail was very small and some samples were even below the detection limit, the changes in percentage were apparent. In numeric terms, the changes in EC by replacement of B5 were between -0.09 to 0.22 mg/kg. Zhang et al. (2011) studied two biodiesels: waste cooking oil and soybean oil, both biodiesels showed an increase in OC and a decrease in EC. Lu et al. (2012) reported that the use of WCO-based biodiesel could effectively decrease EC emission. They explained that the lower volatility of unburnt biodiesel may promote particles nucleation and condensation when the exhaust in the tailpipe being cooled down, leading to a higher OC emission (Lu et al. 2012). This study shared the same observation with previous studies about an increase in OC. Statistically significances (Student's t-test, $p < 0.05$) were observed for the increase in TC and OC during steady-state test by applying B5. Although a large percentage change in both positive and negative in EC when using B5 were recorded, there were large standard deviations since there was single trial with a detectable record in certain driving cycles. Therefore, there were minimal emissions in OC or EC, and the effect of B5 on EC were statistically insignificant. In this study a very high OC proportion and an increase in OC emission were observed, it should be noted that the determination of OC by a quartz filter may be affected by both positive and negative artifacts. Eatough et al (1993) stated that the losses of organic compounds on a filter due to volatilization during and after sampling can be significant. On the other hand, the filter may retain vapor phase organic compounds through adsorption during sampling (Appel et al., 1983).

3.2. PAHs and oxy-PAHs

30 PAHs and 10 oxy-PAHs were quantified from the particulate emissions. Among the tested PAHs, it was found that the levels of 2 PAH species (i.e., Retene and Picene) were lowered than the detection limits. Figure 3 shows the *EF*s of PAHs and oxy-PAHs in different driving conditions with B0 and B5. The *EF*s of total PAHs ranged from 58.9 ± 14.4 to 137.9 ± 71.9 μg/kg with B5. The use of B5 exhibited 50.2% reduction of total PAHs emissions over NEDC, compared

to B0. For steady-state and idling, there was a 30.7% and 15.2% reduction, respectively, when replacing B0 by B5. It was found that the highest *EF*s of PAHs and oxy-PAHs occurred in idling cycles for both B0 and B5. There was a statistically significance (Student's t-test, $p < 0.05$) for the effect of B5 blend on total PAHs *EFs* over NEDC.

Table 4 lists the averaged *EF*s of the analyzed PAHs and Table 5 lists the average *EFs* of oxy-PAHs under three different driving conditions. It was found that the *EF*s of total PAHs were dominantly attributed to low molecular weight (LMW-, 2 to 3ring) PAHs including Acenaphthylene (ACY), Acenaphthene (ACE), Fluorene (FL), and Naphthalene (NAP). Together, they contributed to around 70% of the total particle-phase PAHs when B0 was used. It should be noted that these species have high volatility, and the results could be affected by temperature as well as other conditions. It was found that there was a reduction in total *EF*s of these dominant LMW-PAHs by 61.1% in NEDC, 47.7% in steady-state, and 28.4% in idling, respectively, when replacing B0 by B5. Other 3-ring PAHs such as Anthracene (ANT), Phenanthrene (PA) and 9-Methylanthracene (9-ANT), were also reduced substantially. All LMW-PAH were reduced over NEDC with B5. Some 2-ring PAHs such as 2,6-Dimethylnaphthalene (2,6-NAP) and 2-Methylnaphthalene (2-NAP) were increased in steady-state and idling cycles. With the application of B5 the *EF*s of LMW-PAHs were decreased by 59.1% in NEDC, 44.7% in steady-state, and 27.7% in idling, respectively, when compared to B0. Several previous studies reported that the emission of LMW-PAHs was originated from condensation of unburnt diesel or lubricating oil, or pyrolyzed from incomplete fuel combustion (Ballesteros et al., 2010; Lu et al., 2012; De Souza & Corrêa, 2017). The higher oxygen content in biodiesel blend could induce more complete combustion, which could be a possible reason of the decreased *EF*s of total PAHs and LMW-PAHs over all three driving conditions with the application of B5.

It was found that high molecular weight (HMW-, 5- to 7-ring) and medium molecular weight (MMW-, 4-ring) PAHs did not show a reduction trend when substituted by B5. The *EF*s of

MMW-PAHs were lowered by 31.1% in NEDC with B5. However, the *EFs* were increased by 33.9% and 5.2% over idling, and steady-state cycle, respectively. Pyrene (Pyr) was reduced in all driving conditions, but other 4-ring species were mostly increased over steady-state and idling. On the other hand, four of the six tested MMW-PAHs with relatively lower molecular mass were decreased in NEDC. All HMW-PAH species were increased in idling test with the application of B5; most HMW-PAH species were increased in NEDC and steady-state cycles except Benzo[*k*]fluoranthene (BkF) and Benzo[*b*]fluoranthene (BbF) in NEDC and steady-state cycles, as well as Dibenzo[*a,e*]pyrene (DBP) in NEDC. Ballesteros et al. (2010) suggested that the elevated levels of HMW-PAHs emitted from the diesel engine were mainly formed by combustion reaction through pyrosynthesis of the fuel fragments. Besides, the unsaturated components in biodiesel may enhance flame temperatures and promote the formation of heavier PAHs (Cheung et al., 2010).

The oxy-PAHs *EF*s ranged from 2.2 ± 0.6 to 4.3 ± 2.5 μg/kg with B5 which only contributed to a small fraction of the total PAHs. There was an increase in the *EF*s of oxy-PAHs by 12.1% in steady-state, but in NEDC and idling tests there was a reduction by 27.0% and 3.8%, respectively, by using B5 instead of B0. It was found that 1,4-Naphthoquinone (1,4-NQ) was the most dominant oxy-PAH species with B0 and contributed almost half of the total oxy-PAHs *EF*s. By using B5, the level of emitted 1,4-NQ was reduced significantly over all driving conditions (i.e., 53.6% - 71.9%) which contributed to the total oxy-PAHs emission reduction. 7 of 10 analyzed oxy-PAHs, which were all 3- to 4-rings species, were observed increasing in all driving conditions. Generally, using B5 reduced the *EF*s of 2- to 3-ring oxy-PAHs but increased the *EF*s of 4- and 5-ring oxy-PAHs.

Individual PAH species with different number of rings or molecular weight changed differently with B5, which showed that the two fuel blends caused different exhaust compositions of PAHs. Figure 4 shows the contribution of each PAH species to the total. With the application of B5, the contribution of 2- and 3-ring PAHs and 2-ring oxy-PAHs to total *EFs* dropped, while the share of the other PAHs and oxy-PAHs increased, compared with B0. The contribution of LMW-PAHs shrank from 83.6% to 68.9% in average across the three driving conditions. PAHs with higher molecular weights increased their share in total emissions. On average, the contribution of the sum of MMW-PAHs and HMW-PAHs together increased from 13.8% to 27.5%, and the contribution of oxy-PAHS increased from 2.6% to 3.6%.

3.3. Comparison of PAHs and oxy-PAHs results with literature

This study observed a reduction of total particle phase PAHs and LMW-PAHs with biodiesel blend, which is consistent with previous studies. Guan et al. (2017) reported a trend of increasing suppression of total PAHs with the increase of biodiesel content. This study agrees with previous studies that the particle-phase PAH emission profiles were dominant in PAHs with lower molecular weight, and had low abundance in HMW-PAHs, in diesel and biodiesel exhausts (He et al., 2010; Karavalakis et al., 2011; Lu et al., 2012; De Souza & Corrêa, 2016).

In addition to literature that the tests were based on diesel engine, the effects of biodiesel on exhaust were tested on some other types of vehicles. Karavalakis et al. (2017) compared diesel with B50 blend of methyl ester from soybran oil, waste cooking oil, and animal fat on heavy duty diesel vehicles, and found that the total PAHs emissions with all biodiesel blends were lower than those when using diesel. Zhang et al. (2019) tested WCO-based biodiesel in low level blends (B5, B10, and B20) on a bus and reported a reduction in total PAHs, as well as a shift in PAH composition from 3-ring PAHs to PAHs with more rings, at all blend levels. Opposite results were also reported by several studies. Frying oil methyl ester in low level blends (B10, B20, and B30) for a passenger car, and in mid-high level blends (B30, B50, and B80) for a light duty vehicle were investigated by Karavalakis et al. (2011) and Bakeas et al. (2011a), respectively. In both studies these biodiesel blends resulted in a higher total PAHs, light PAHs, and oxy-PAHs. They suggested that the di-esters formed in parent oil during thermal stressing could ultimately present in final fuel and exhaust. They also pointed out that unsaturated and oxidized biodiesel may promote PAHs emissions because the formation of hydroperoxides during oxidation would ultimately decompose to aldehydes and higher molecular weight species.

Despite the agreement between this study and the majority of previous studies that PAHs decreased with biodiesel and there was a higher proportion of LMW-PAHs, the composition of PAHs species was observed variable among different studies. For instance, NAP accounted for the highest proportion in particle PAH species in current study and the study of Huang et al. (2015), but some studies (e.g. Lu et al., 2012; He et al., 2010; De Abrantes et al., 2004) reported a lower share of NAP in particle phase than other species such as ANT, PA, PYR, and FL. One of the possible reasons is that some part of the gas phase NAP was absorbed on quartz filters, which could affect the NAP levels detected.

Guan et al. (2017) tested the WCO-based biodiesel blends (20% or 50% biodiesel; and 10% biodiesel with 5% or 10% ethanol) and reported an increase in oxy-PAHs emissions from a diesel engine. Karavalakis et al. (2010) reported an increase in oxy-PAHs emissions despite a reduction in total PAHs from soy-based biodiesel (10% biodiesel). In contrast to previous studies which suggested biodiesel may enhance oxy-PAHs formation, current study observed a reduction in oxy-PAHs in both idling and NEDC cycles. Heavier oxy-PAHs generally had higher emissions when using B5, attributing to their stable fragment structures (Barbella et al., 1989). In the study from Guan et al. (2017), the level of 1,4-NQ was reported to increase with the biodiesel content. Karavalakis et al. (2010) tested a Euro II passenger car without a DPF and 1,4-NQ was excluded from their study. The difference in engine types, fuels, and PAHs species being measured may cause the disagreement in oxy-PAHs results. Nonetheless, this study observed that the oxy-PAHs had a higher share in PAH constitution and a rise in 4- and 5-ring oxy-PAHs with B5.

Several studies have tested the effect of biodiesel blends made from different raw materials. For example, Karavalikis et al. (2010; 2011) reported that used frying oil methyl ester has a lower total PAH emission than diesel and biodiesel blend from soybean oil, palm oil, sunflower oil, and rapeseed oil; but a higher emission than biodiesel blend from animal fat, olive oil, and a blend from soybean and palm oil, when a low blend level (B10) was tested on passenger cars under NEDC. The relative changes of exhaust emissions were depending on driving cycles.

3.4. Toxicity of PAHs and oxy-PAHs emissions

Figure 5 presents the contribution of individual species to the overall BaP_{eq} *EF*s with B0 and B5 fuels. With B5, the BaP_{eq} *EF*s were 3.10 ± 0.76 (NEDC), 3.34 ± 2.17 (steady-state), and 5.89 ± 2.55 μg/kg (idling), respectively. The BaP_{eq} *EF*s for B5 were increased by 11.3% in NEDC, 53.8% in steady-state, and 117.0% in idling tests, respectively, compared to B0. It was found that the majority of toxicity came from benzo[*a]*pyrene (BaP) and dibenzo[*a,h*]anthracene (DBA), which also had the highest TEF.

The TEFs of individual PAH are listed in Table 6 together with their BaP_{eq} *EF*s for B0 and B5 fuels over different driving cycles in Figure 5. The use of B5 led to higher BaP_{eq} *EF*s than those for B0, reflecting its higher toxicity of PAH emissions. This was mainly attributed to the increased emissions of HMW-PAHs such as Dibenzo[*a,h*]anthracene (DBA), Benzo[*a]*pyrene (BaP), and Indeno[1,2,3-c,d]pyrene (IND). In particular, the use of B5 led to a 26.8% (NEDC), 70.3% (steady-state), and 105.2% (idling) increase of BaP *EF*s, respectively, as compared to B0. While the total PAH *EF*s were reduced when B5 was used, the HMW-PAHs *EF*s increased and the TEF for some HMW-PAHs were higher than that for LMW-PAHs (particularly BaP and DBA), resulting in an overall increase of toxicity. As these compounds are carcinogenic, this raises concerns of the public health regarding the application of biodiesel.

This study estimated the toxicity based on 16 particulate PAHs prioritized by U.S. Environmental Protection Agency, which may underrepresent the carcinogenic potency from the complete gaseous and particulate PAHs (Samburova et al., 2017). Furthermore, many oxy-PAHs are genotoxic and mutagenic. Among the oxy-PAHs species being examined in this study, Benzo[*a*]anthracene-7,12-dione (BaA7,12-dio), 6H-Benzo[*c,d*]pyrene-6-one (6H-BcdP-6-one), and 5,12-Naphthacenequinone (5,12-NACQ) were three of the four major oxy-PAHs suggested to be prioritized for toxicological research for them being mutagenic, tumor promoters, and/or enzymatic inductors (Clergé et al., 2019). The application of B5 led to an increase in 5,12-NACQ in a range between 26.0% and 131.4%; and an increase in BaA7,12-dio in a range between 80.7% and 144.3%. 6H-BcdP-6-one, on the other hand, was only increased during idling, by 3.9%. While the increase in $\mathrm{BaP_{eq}}$ *EFs* was not statistically significant, it is suggested to comprehensively study the toxicity from PAHs and oxy-PAHs and look for solutions to address the toxicity issue of biodiesel blend application.

4. Conclusion

This study evaluates the particle emissions from a Euro VI-LDV when with B0 and B5. Driving cycle has a huge influence on the effect of B5 blend application. A domination of OC over EC was noticed in OC/EC analysis for all combinations of driving cycles and fuel blends, suggesting that the particulate matter, especially EC, could be removed effectively by the DPF. The *EF*s of OC were raised by 30% in NEDC, 23% in steady-state, and 111% in idling test, respectively, when using B5 instead of B0.

Under all driving conditions, the B5 fuel reduced emissions of total particulate phase PAHs, the *EF* was reduced by 50% in NEDC, 31% in steady-state, and 15% in idling, respectively. The drop was attributed to the decrease in 3-ring PAH *EF*s. Other PAHs with a larger molecular mass usually experienced an increase in *EF*s. The PAH profile of B5 was also different from that of B0, in that the share of PAH and oxy-PAHs with low molecular weight decreased while the other groups rose. Despite the reduction of PAH *EF*s, the toxicity from PAHs expressed as $\mathrm{BAP_{eq}}$ *EF*s was higher when B5 was used due to the change in PAH composition. It was increased by 2.2 times in NEDC and steady-state tests, and 2.6 times at idling test. Although the use of B5 WCO-based biodiesel blend could enhance sustainability compared to diesel fuel, the results of this study raise atmospheric and health concern, since there was a higher OC emission and toxicity from PAHs with biodiesel blend. This study contributes to the comprehensive understanding of the feasibility of using biodiesel blends in Hong Kong.

Acknowledgements

The work described in this paper was supported by a grant from the Research Grants Council of HKSAR, China (UGC/FDS/25/E01/18).

References

Abrantes, R., Assuncao, J. V., Pesquero, C. R., Bruns, R. E., Nobrega, R. B., 2009. Emission of polycyclic aromatic hydrocarbons from gasohol and ethanol vehicles. Atmospheric Environment 43, 648–654.

Agarwal, A. K., Gupta, T., Dixit, N., Shukla, P. C., 2013. Assessment of toxic potential of primary and secondary particulates/aerosols from biodiesel vis-a-vis mineral diesel fuelled engine. Inhalation Toxicol 25, 325–32.

Appel, B. R., Tokiwa, Y., Kothny, E. L., 1983. Sampling of carbonaceous particles in the atmosphere. Atmospheric Environment 17(9), 1787-1796.

Bakeas, E., Karavalakis, G., Fontaras, G., Stournas, S., 2011a. An experimental study on the impact of biodiesel origin on the regulated and PAH emissions from a Euro 4 light-duty vehicle. Fuel, 90(11), 3200-3208.

Bakeas, E., Karavalakis, G., Stournas, S., 2011b. Biodiesel emissions profile in modern diesel vehicles. Part 1: Effect of biodiesel origin on the criteria emissions. Science of the Total Environment 409(9), 1670-1676.

Ballesteros, R., Hernández, J. J., Lyons, L. L., 2010. An experimental study of the influence of biofuel origin on particle-associated PAH emissions. Atmospheric Environment 44(7), 930-938.

Barbella, R., Ciajolo, A., d'Anna, A., Bertoli, C., 1989. Effect of fuel aromaticity on diesel emissions. Combustion and Flame 77(3-4), 267-277.

Chen, F., Hu, W., Zhong, Q., 2013. Emissions of particle-phase polycylic aromatic hydrocarbons (PAHs) in the Fu Gui-shan tunnel of Nanjing, China. Atmospheric Research 124, 53–60.

Cheung, K. L., Ntziachristos, L., Tzamkiozis, T., Schauer, J. J., Samaras, Z., Moore, K. F., Sioutas, C., 2010. Emissions of particulate trace elements, metals, and organic species from gasoline, diesel, and biodiesel passenger vehicles and their relation to oxidative potential. Aerosol Science and Technology 44(7), 501-513.

Chow, J. C., Watson, J. G., Chen, L. W. A., Chang, M. C. O., Robinson, N. E., Trimble, D., Kohl, S., 2007. The IMPROVE_A temperature protocol for thermal/optical carbon analysis: Maintaining consistency with a long-term database. Journal of the Air & Waste Management Association 57(9), 1014-1023.

Clergé, A., Goff, J. L., Lopez, C., Ledauphin, J., Delépée, R., 2019. Oxy-Pahs: occurrence in the environment and potential genotoxic/mutagenic risk assessment for human health. Critical Reviews in Toxicity 39(6), 1-21.

De Abrantes, R., De Assunção, J. V., R. Pesquero, C., 2004. Emission of polycyclic aromatic hydrocarbons from light-duty diesel vehicles exhaust. Atmospheric Environment 38(11), 1631-1640.

De Souza, C. V., Corrêa, S. M., 2016. Polycyclic aromatic hydrocarbons in diesel emission, diesel fuel and lubricant oil. Fuel 185, 925-931.

Dynamic Progress International Limited, 2012. Material Safety Data Sheet for B100 Biodiesel. Retrieved from http://www.dynamic-progress.com.hk/products_services.php?action=details&nid=9, (assessed 1 September 2020).

Eatough, D. J., Wadsworth, A., Eatough, D. A., Crawford, J. W., Hansen, L. D., Lewis, E. A., 1993. A multiple-system, multi-channel diffusion denuder sampler for the determination of fine-particulate organic material in the atmosphere. Atmospheric Environment 27(8), 1213-1219.

Fraser, M. P., Lakshmanan, K., Fritz, S. G., Ubanwa, B., 2002. Variation in composition of fine particulate emissions from heavy-duty diesel vehicles. Journal of Geophysical Research 107 (D21), 8346.

Guan, C., Cheung, C. S., Li, X., Huang, Z., 2017. Effects of oxygenated fuels on the particule-phase compounds emitted from a diesel engine. Atmospheric Pollution Research 8(2), 209-220.

He, C., Ge, Y., Tan, J., You, K., Han, X., Wang, J., 2010. Characteristics of polycyclic aromatic hydrocarbons emissions of diesel engine fueled with biodiesel and diesel. Fuel 89(8), 2040-2046.

Ho, S. S. H., Yu, J. Z., Chow, J. C., Zielinska, B., Watson, J. G., Sit, E. H. L., Schauer, J. J., 2008. Evaluation of an in-injection port thermal desorption-gas chromatography/mass spectrometry method for analysis of non-polar organic compounds in ambient aerosol samples. Journal of Chromatography A 1200, 217-227.

Huang, L., Bohac, S. V., Chernyak, S. M., Batterman, S. A., 2015. Effects of fuels, engine load and exhaust after-treatment on diesel engine SVOC emissions and development of SVOC profiles for receptor modeling. Atmospheric Environment 102, 228-238.

IARC, 2012. Diesel and Gasoline Engine Exhausts and Some Nitroarenes Monographs on the Evaluation of Carcinogenic Risks to Humans, Lyon, France, Volume 105.

Karavalakis, G., Fontaras, G., Ampatzoglou, D., Kousoulidou, M., Stournas, S., Samaras, Z., Bakeas, E., 2010. Effects of low concentration biodiesel blends application on modern passenger cars. Part 3: Impact on PAH, nitro-PAH, and oxy-PAH emissions. Environmental Pollution 158(5), 1584-1594.

Karavalakis, G., Boutsika, V., Stournas, S., Bakeas, E., 2011. Biodiesel emissions profile in modern diesel vehicles. Part 2: Effect of biodiesel origin on carbonyl, PAH, nitro-PAH and oxy-PAH emissions. Science of the Total Environment 409(4), 738-747.

Karavalakis, G., Johnson, K. C., Hajbabaei, M., Durbin, T. D., 2016. Application of low-level biodiesel blends on heavy-duty (diesel) engines: Feedstock implications on NO_x and particulate emissions. Fuel 181, 259-268.

Karavalakis, G., Gysel, N., Schmitz, D. A., Cho, A. K., Sioutas, C., Schauer, J. J., Cocker, D. R., Durbin, T. D., 2017. Impact of biodiesel on regulated and unregulated emissions, and redox and proinflammatory properties of PM emitted from heavy-duty vehicles. Science of the Total Environment 584-585, 1230-1238.

Knothe, G., Razon, L. F., 2017. Biodiesel fuels. Progress in Energy and Combustion Science 58, 36-59.

Lapuerta, M., Armas, O., Rodriguez-Fernandez, J., 2008. Effect of biodiesel fuels on diesel engine emissions. Progress in Energy and Combustion Science 34, 198-223.

Lu, T., Huang, Z., Cheung, C. S., Ma, J., 2012. Size distribution of EC, OC and particle-phase PAHs emissions from a diesel engine fueled with three fuels. Science of the Total Environment 438, 33-41.

Man, X. J., Cheung, C. S., Ning, Z., Wei, L., Huang, Z. H., 2016. Influence of engine load and speed on regulated and unregulated emissions of a diesel engine fueled with diesel fuel blended with waste cooking oil biodiesel. Fuel 180,41-49.

Maria del Rosario Sienra, M., 2006. Oxygenated polycyclic aromatic hydrocarbons in urban air particulate matter. Atmospheric Environment 40, 2374-2384.

Na, K., Biswas, S., Robertson, W., Sahay, K., Okamoto, R., Mitchell, A., Lemieux, S., 2015. Impact of biodiesel and renewable diesel on emissions of regulated pollutants and greenhouse gases on a 2000 heavy duty diesel truck. Atmospheric Environment 107, 307 -314

Nisbet, I. C. T., LaGoy, P. K., 1992. Toxic equivalency factors (TEFs) for polycyclic aromatic-hydrocarbons (PAHs). Regulatory Toxicology Pharmacology 16, 290-300.

Panel on Environmental Affairs, Legislative Council of the Hong Kong Special Administrative Region of the People's Republic of China, 2018. Administration's paper on progress on improving roadside air quality. Available at: https://www.legco.gov.hk/yr18-19/english/panels/ea/papers/ea20181219cb1-319-4-e.pdf, (accessed September 2020).

Samburova, V., Zielinska, B., Khlystov, A., 2017. Do 16 polycylic aromatic hydrocarbons represent PAH air toxicity? Toxic 5(3), 17.

Shah, S. D., Cocker, D. R., Miller, J. W., Norbeck, J. M. 2004. Emission rates of particulate matter and elemental and organic carbon from in-use diesel engines. Environmental Science & Technology 38(9), 2544-2550.

Shen, H. Z., Tao, S., Wang, R., Wang, B., Shen, G. F., Li, W., Su, S. S., Huang, Y., Wang, X. L., Liu, W. X., Li, B. G., Sun, K., 2011. Global time trends in PAH emissions from motor vehicles. Atmospheric Environment 45, 2067–2073.

Shibata, K., Enya, K., Ishikawa, N., Sakamoto, K., 2019. EC/OC and PAHs Emissions from a Modern Diesel Engine with DPF Regeneration Fueled by 10% RME Biodiesel. Aerosol and Air Quality Research 19, 1765-1774.

The Government of the Hong Kong Special Administrative Region, 2019. Press release: LCQ12: Promoting use of biodiesel, https://www.info.gov.hk/gia/general/201906/05/P2019060500435.htm, (accessed 3 July 2021).

Tomaz, S., Jaffrezo, J. L., Favez, O., Perraudin, E., Villenace, E., Albinet, A., 2017. Sources and atmospheric chemistry of oxy- and nitro-PAHs in the ambient air of Grenoble (France). Atmospheric Environment 161, 144-154.

Tsai, J. H., Chen, S. J., Huang, K. L., Lin, Y. C., Lee, W. J., Lin, C. C., Lin, W. Y., 2010. PM, carbon, and PAH emissions from a diesel generator fueled with soy-biodiesel blends. Journal of Hazardous Materials 179, 237-243.

U.S. Environmental Protection Agency (USEPA), 2002. Health assessment document for diesel engine exhaust. Prepared by the National Center for Environmental Assessment, Washington, DC, for the Office of Transportation and Air Quality; EPA/600/8-90/057F. Available from: National Technical Information Service, Springfield, VA; PB2002-107661, and <http://www.epa.gov/ncea>.

Walgraeve, C., Chantara, S., Sopajaree, K., De Wispelaere, P., Demeestere, K., Van Langenhove, H., 2015. Quantification of PAHs and oxy-PAHs on airborne particle matter in Chiang Mai, Thailand, using gas chromatography high resolution mass spectrometry. Atmospheric Environment 107, 262-272.

Wang, B., Lau, Y. S., Huang, Y., Organ, B., Chuang, H. C., HO, S. S. H., Qu, L., Lee, S. C., Ho, K. F. 2021. Chemical and toxicological characterization of particulate emissions from diesel vehicles. Journal of Hazardous Materials 405, 124613.

Williams, A., McCormick, R. L., Hayes, R. R., Ireland, J., Fang, H. L., 2012. Effect of biodiesel blends on diesel particulate filter performance. SAE Technical Paper 2012-01-1666. Available at: https://doi.org/10.4271/2012-01-1666, (accessed September 2020).

Zhang, J., He, K., Shi, X., Zhao, Y., 2011. Comparison of Particle Emissions from an Engine Operating on Biodiesel and Petroleum Diesel. Fuel 90 (6), 2089-2097.

Zhang, H., Magara-Gomez, K. T., Olson, M. R., Okuda, T., Walz, K. A., Schauer, J. J., Kleeman, M. J., 2015. Atmospheric impacts of black carbon emission reductions through the strategic use of biodiesel in California. Science of the Total Environment 538, 412-422.

Zhang, J., He, K., Shi, X., Zhao, Y., 2009. Effect of SME biodiesel blend on $PM_{2.5}$ emission from a heavy-duty engine. Atmospheric Environment 43, 2442-2448.

Zhang, Y., Lou, D., Hu, Z., Tan, P., 2019. Particle number, size distribution, carbons, polycyclic aromatic hydrocarbons and inorganic ions of exhaust particles from a diesel bus fueled with biodiesel blends. Journal of Cleaner Production 225, 627-636.

Table 1: The specification of the tested Euro-VI light duty diesel vehicle.

Parameter	Value	Parameter	Value
Emission level:	**Euro VI**	Engine type:	**2.5D WGT diesel engine (turbocharger)**
Place of manufacture:	**Hyundai**	Engine size/ displacement (L):	**2.497**
Model:	**H1**	Maximum power:	**100kW / 3800 rpm**
Year of registration:	**2019**	Maximum torque:	**343Nm/1500-2500 rpm**
Vehicle weight (kg):	**2000**	Exhaust emission control:	**DOC, DPF, EGR, LNT**
No. of cylinders:	**4**	Pre-test odometer reading (km):	**77**
Transmission:	**6 MT**		

Table 2: The properties of the tested fuels (Dynamic Progress International Limited, 2012; Man et al., 2016).

		Biodiesel (B100) (Dynamic Progress Int. Ltd)	Ultralow sulphur content diesel (B0)
Physical properties			
Cetane Index		51	52
Heat of evaporation	(kJ/kg)	300	250–290
Lower heating value	(MJ/kg)	37.5	42.5
Density at 20°C	(kg/m)	871	840
Vapour point at 25 °C	(mmHg)	< 2	NA
Viscosity at 40 °C	(mPa•s)	4.6	2.4
Chemical properties			
Carbon/Hydrogen/Oxygen	(wt%)	77.1/12.1/10.8	86.6/13.4/0

Table 3: The FAMEs contents of the neat WCO based biodiesel (B100) manufactured by Dynamic progress Ltd, with reference to the statistical analysis of the FAMEs contents of WCO based biodiesel (Giakourmis 2013; Man et al., 2016).

Fatty acid methyl ester contents (w.t. %)		**GC results (Man et al., 2016)**	**Statistical results (Giakourmis, 2013)**
Tridecanoic	(C13:0)	1.12	NA
Myristic	(C14:0)	1.11	0.67
Palmitic	(C16:0)	11.46	15.69
Palmitoleic	(C16:1)	0.60	0.73
Stearic	(C18:0)	4.22	6.14
Oleic	(C18:1)	35.22	42.84
Linoleic	(C18:2)	39.73	29.36
Linolenic	(C18:3)	6.24	2.03
Lignoceric	(C24:0)	0.30	NA

Table 4: Summary of fuel-based *EFs* of PAHs (µg/kg). Values are mean ± S.D.

Driving test			**NEDC**		**Steady-state**		**Idling**	
Fuel test			**B0**	**B5**	**B0**	**B5**	**B0**	**B5**
PAHs	**Abbreviation**	**No. of aromatic rings**	**Fuel-based emission factor (µg/kg)**					
Naphthalene	NAP	2	22.69 ± 0.52	15.12 ± 3.71	18.66 ± 4.45	16.86 ± 11.93	40.17 ± 22.17	39.04 ± 17.69
1-Methylnaphthalene	1-NAP	2	2.66 ± 0.43	2.24 ± 0.29 *	2.09 ± 0.74	2.22 ± 1.47	4.23 ± 3.28	4.13 ± 2.03
2-Methylnaphthalene	2-NAP	2	2.59 ± 0.14	2.29 ± 0.69	1.87 ± 0.13	2.41 ± 1.70	4.07 ± 2.88	5.01 ± 3.73
2,6-Dimethylnaphthalene	2,6-NAP	2	1.89 ± 0.71	1.75 ± 0.26	1.50 ± 0.91	1.73 ± 1.01	2.54 ± 1.22	3.04 ± 1.22
Acenaphthylene	ACY	3	15.42 ± 3.10	6.41 ± 1.74	13.70 ± 6.32	6.61 ± 4.42	21.80 ± 6.50	16.82 ± 9.78
Acenaphthene	ACE	3	18.70 ± 5.28	5.99 ± 1.71 *	15.48 ± 5.35	6.04 ± 4.07	24.83 ± 4.81	18.75 ± 14.57
Fluorene	FL	3	23.08 ± 5.28	3.54 ± 1.47 *	16.51 ± 8.11	4.17 ± 2.76	31.69 ± 4.98	10.18 ± 5.74 *
Anthracene	ANT	3	4.03 ± 0.58	0.79 ± 0.26 *	3.37 ± 0.94	0.98 ± 0.70 *	4.37 ± 2.24	1.44 ± 0.79
Phenanthrene	PA	3	3.64 ± 0.66	0.80 ± 0.32 *	2.96 ± 0.81	1.07 ± 0.78 *	3.45 ± 0.93	1.38 ± 0.70*
9-Methylanthracene	9-ANT	3	1.97 ± 0.12	0.64 ± 0.23 *	1.28 ± 0.37	0.68 ± 0.45	2.58 ± 1.31	1.20 ± 0.70
Retene	RET	3	<LOD	<LOD	<LOD	<LOD	<LOD	<LOD
Pyrene	PYR	4	2.67 ± 0.49	0.91 ± 0.39 *	1.91 ± 0.46	0.98 ± 0.70	2.48 ± 1.01	1.72 ± 0.97
Fluoranthene	FLA	4	1.94 ± 0.36	1.12 ± 0.37	1.28 ± 0.82	1.52 ± 1.15	1.96 ± 0.47	2.62 ± 1.21
Methylfluoranthene	Mt-FLA	4	0.94 ± 0.06	0.80 ± 0.22	0.63 ± 0.25	0.81 ± 0.61	1.27 ± 0.67	1.62 ± 1.06
Benzo[*a*]anthracene	BaA	4	1.18 ± 0.55	0.90 ± 0.15	1.00 ± 0.53	0.98 ± 0.62	1.06 ± 0.12	1.79 ± 0.79
Chrysene	CHR	4	1.53 ± 0.50	1.74 ± 0.25	1.12 ± 0.41	1.81 ± 1.31	1.32 ± 0.16	2.93 ± 1.62
Methylchrysene	Mt-CHR	4	0.32 ± 0.06	0.45 ± 0.11	0.23 ± 0.09	0.40 ± 0.19	0.51 ± 0.24	0.83 ± 0.37
Cyclopenta[*c,d*]pyrene	CPcdPYR	5	0.72 ± 0.28	1.09 ± 0.38	0.46 ± 0.13	1.50 ± 1.22	1.05 ± 0.39	2.19 ± 1.52
Benzo[*a*]fluoranthene	BaF	5	0.37 ± 0.06	0.56 ± 0.12	0.29 ± 0.09	0.51 ± 0.35	0.31 ± 0.09	0.94 ± 0.54
Benzo[*a*]pyrene	BaP	5	0.64 ± 0.07	0.82 ± 0.15	0.51 ± 0.05	0.87 ± 0.58	0.64 ± 0.30	1.32 ± 0.61
Benzo[*b*]fluoranthene	BbF	5	0.85 ± 0.10	0.46 ± 0.13	0.65 ± 0.14	0.56 ± 0.40	0.85 ± 0.21	0.91 ± 0.53
Benzo[*e*]pyrene	BeP	5	0.28 ± 0.03	0.32 ± 0.04	0.24 ± 0.04	0.38 ± 0.27	0.31 ± 0.12	0.56 ± 0.22
Benzo[*k*]fluoranthene	BkF	5	1.03 ± 0.23	0.54 ± 0.19	0.69 ± 0.30	0.58 ± 0.41	0.80 ± 0.23	0.89 ± 0.45
Perylene	PER	5	0.22 ± 0.01	0.24 ± 0.06	0.18 ± 0.04	0.26 ± 0.15	0.21 ± 0.06	0.40 ± 0.15
PIcene	PIC	5	<LOD	<LOD	<LOD	<LOD	<LOD	<LOD
Dibenzo[*a,h*]anthracene	DBA	5	1.58 ± 0.38	1.83 ± 0.50	1.22 ± 0.37	1.96 ± 1.27	1.50 ± 0.32	3.69 ± 1.56
Indeno[*1,2,3-c,d*]pyrene	IND	6	1.07 ± 0.05	1.93 ± 0.64	0.83 ± 0.12	2.28 ± 1.46	1.09 ± 0.30	3.68 ± 1.55
Benzo[*g,h,i*]perylene	BghiP	6	0.66 ± 0.17	0.84 ± 0.08	0.51 ± 0.25	1.04 ± 0.63	0.66 ± 0.24	1.37 ± 0.43 *
Dibenzo[*a,e*]pyrene	DBP	6	1.88 ± 0.32	1.72 ± 0.63	1.30 ± 0.33	2.00 ± 1.33	1.80 ± 0.27	3.94 ± 2.02
Coronene	COR	7	0.57 ± 0.11	0.83 ± 0.17	0.49 ± 0.21	0.83 ± 0.53	0.59 ± 0.33	1.19 ± 0.32 *
Sum of PAHs			**115.16 ± 16.22**	**56.68 ± 13.84***	**90.97 ± 24.92**	**62.03 ± 40.75**	**158.17 ± 46.48**	**133.61 ± 69.65**

* Indicates significant difference with B5 on total *EFs* compared to B0 (Student's t-test, p<0.05). LOD: limit of detection.
Limit of detection (ng/sample) for Retene is 0.0028; for Picene is 0.0011.

Table 5: Summary of fuel-based *EFs* of oxy-PAHs and total PAHs (μg/kg). Values are mean ± S.D.

Driving test			**NEDC**		**Steady-state**		**Idling**	
Fuel test			**B0**	**B5**	**B0**	**B5**	**B0**	**B5**
Oxy-PAHs	**Abbreviation**	**No. of aromatic rings**	**Fuel-based emission factor (μg/kg)**					
1-Naphthaldehyde	1-NAD	2	0.37 ± 0.03	0.36 ± 0.10	0.27 ± 0.07	0.42 ± 0.26	0.57 ± 0.28	0.64 ± 0.30
1,4-Naphthoquinone	1,4-NQ	2	1.51 ± 0.13	0.43 ± 0.14 *	1.15 ± 0.60	0.54 ± 0.42	2.13 ± 1.02	0.74 ± 0.40
1-Acenaphthenone	1-ACP	3	0.24 ± 0.06	0.29 ± 0.11	0.16 ± 0.04	0.30 ± 0.26	0.30 ± 0.11	0.51 ± 0.39
9-Fluorenone	9-FLO	3	0.18 ± 0.04	0.20 ± 0.07	0.10 ± 0.00	0.25 ± 0.18	0.22 ± 0.09	0.40 ± 0.26
9,10-Anthraquinone	9,10-ANQ	3	0.14 ± 0.01	0.21 ± 0.05	0.14 ± 0.05	0.25 ± 0.15	0.30 ± 0.10	0.44 ± 0.20
1,8-Naphthalic anhydride	1,8-NAPAyd	4	0.20 ± 0.04	0.21 ± 0.07	0.15 ± 0.03	0.27 ± 0.17	0.32 ± 0.09	0.42 ± 0.21
5,12-Naphthacenequinone	5,12-NACQ	4	0.09 ± 0.02	0.12 ± 0.03	0.07 ± 0.03	0.12 ± 0.09	0.12 ± 0.04	0.28 ± 0.26
Benzo[*a*]anthracene-7,12-dione	BaA7,12-dio	4	0.14 ± 0.02	0.25 ± 0.09	0.10 ± 0.03	0.26 ± 0.17	0.20 ± 0.10	0.49 ± 0.33
1,4-Chrysenequinone	1,4-CRQ	4	0.08 ± 0.01	0.09 ± 0.01	0.06 ± 0.03	0.10 ± 0.07	0.13 ± 0.08	0.20 ± 0.13
6H-Benzo[*c,d*]pyrene-6-one	6H-BcdP-6-one	5	0.12 ± 0.03	0.09 ± 0.02	0.09 ± 0.03	0.08 ± 0.05	0.15 ± 0.05	0.16 ± 0.09
Sum of oxy-PAHs			3.07 ± 0.38	2.24 ± 0.60	2.31 ± 0.76	2.59 ± 1.78	4.44 ± 1.74	4.27 ± 2.51
Total PAHs			**118.23 ± 16.59**	**58.92 ± 14.40 ***	**93.27 ± 25.50**	**64.62 ± 42.52**	**162.61 ± 48.21**	**137.88 ± 71.86**

Total PAHs: averaged fuel-based *EFs* of all PAHs and oxy-PAHs.

* Indicates significant difference with B5 on total *EFs* compared to B0 (Student's t-test, $p<0.05$).

Table 6: The TEFs of PAHs and the fuel-based *EF*s (μg/kg) of BaP_{eq}.

Driving test		**NEDC**		**Steady-state**		**Idling**	
Fuel test		**B0**	**B5**	**B0**	**B5**	**B0**	**B5**
PAHs	**TEF**	**BaP_{eq} emission factor (μg/kg)**					
Naphthalene	0.001	0.02	0.02	0.02	0.02	0.04	0.04
Acenaphthene	0.001	0.02	0.01	0.02	0.01	0.02	0.02
Acenaphthylene	0.001	0.01	0.01	0.01	0.01	0.02	0.02
Anthracene	0.01	0.04	0.01	0.03	0.01	0.04	0.01
Fluorene	0.001	0.02	0.00	0.02	0.00	0.03	0.01
Phenanthrene	0.001	0.00	0.00	0.00	0.00	0.00	0.00
Chrysene	0.01	0.02	0.02	0.01	0.02	0.01	0.03
Fluoranthene	0.001	0.00	0.00	0.00	0.00	0.00	0.00
Pyrene	0.001	0.00	0.00	0.00	0.00	0.00	0.00
Benzo[a]anthracene	0.1	0.12	0.09	0.10	0.10	0.11	0.18
Benzo[a]pyrene	1	0.64	0.82	0.51	0.87	0.64	1.32
Benzo[b]fluoranthene	0.1	0.09	0.05	0.07	0.06	0.09	0.09
Benzo[k]fluoranthene	0.1	0.10	0.05	0.07	0.06	0.08	0.09
Dibenzo[a,h]anthracene	1	1.58	1.83	1.22	1.96	1.50	3.69
Benzo[g,h,i]perylene	0.01	0.01	0.01	0.01	0.01	0.01	0.01
Indeno[1,2,3-cd]pyrene	0.1	0.11	0.19	0.08	0.23	0.11	0.37
BaP_{eq} *EF* (μg/kg fuel)		**2.79**	**3.10**	**2.17**	**3.34**	**2.71**	**5.89**
(SD)		(0.48)	(0.76)	(0.52)	(2.17)	(0.68)	(2.56)

TEF: The toxicity equivalent factor developed by Nisbet & LaGoy (1992).

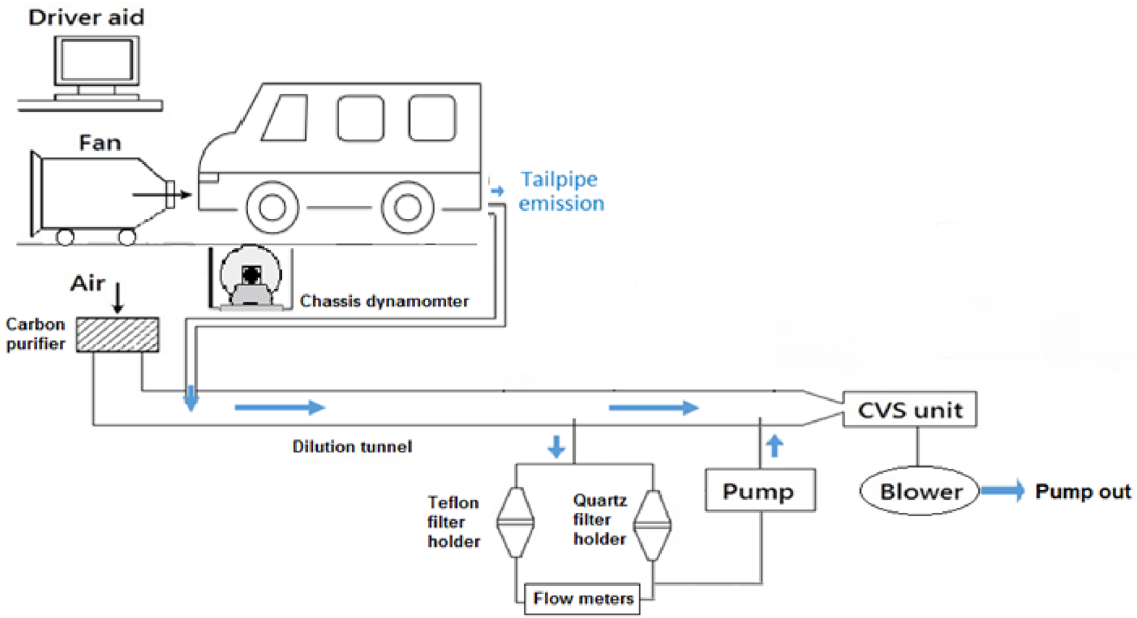

Figure 1: Schematic diagram of the vehicle testing setup.

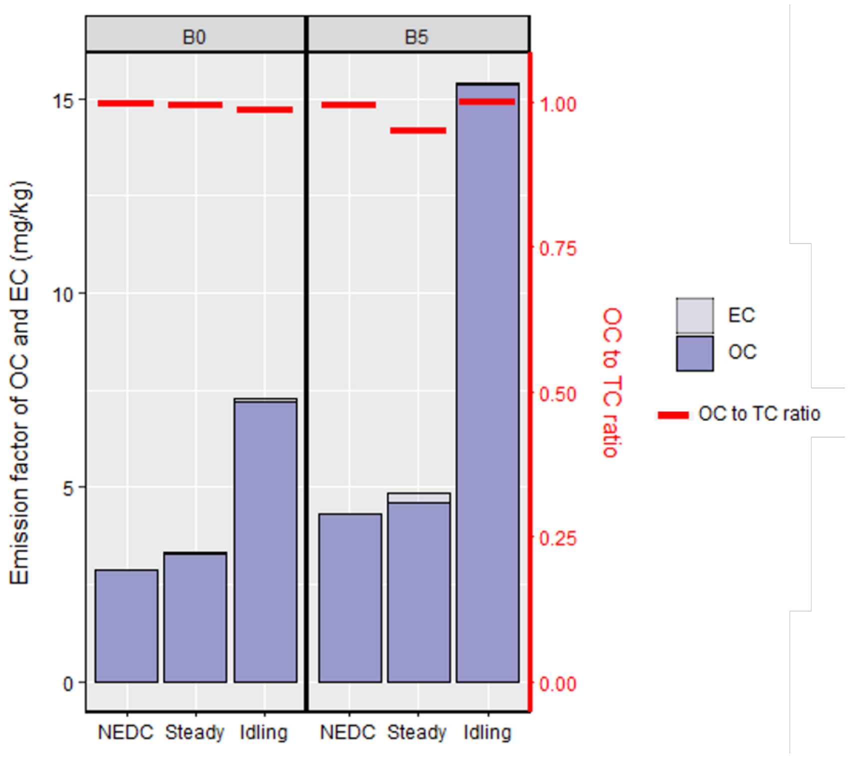

Figure 2: Comparison of fuel-based *EFs* (mg/kg) of OC and EC. Light color bar above presents EC *EF* and deep color bar below represents OC *EF*. The red bars denote the OC to TC ratio.

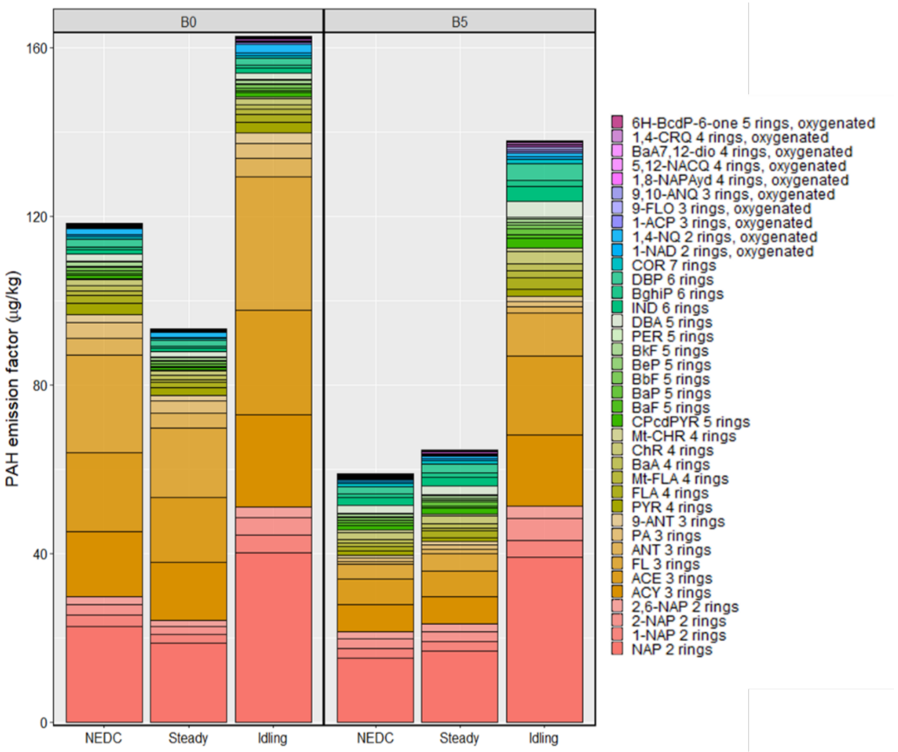

Figure 3: Comparison of average fuel-based *EFs* (µg/kg) of PAH and oxy-PAH species.

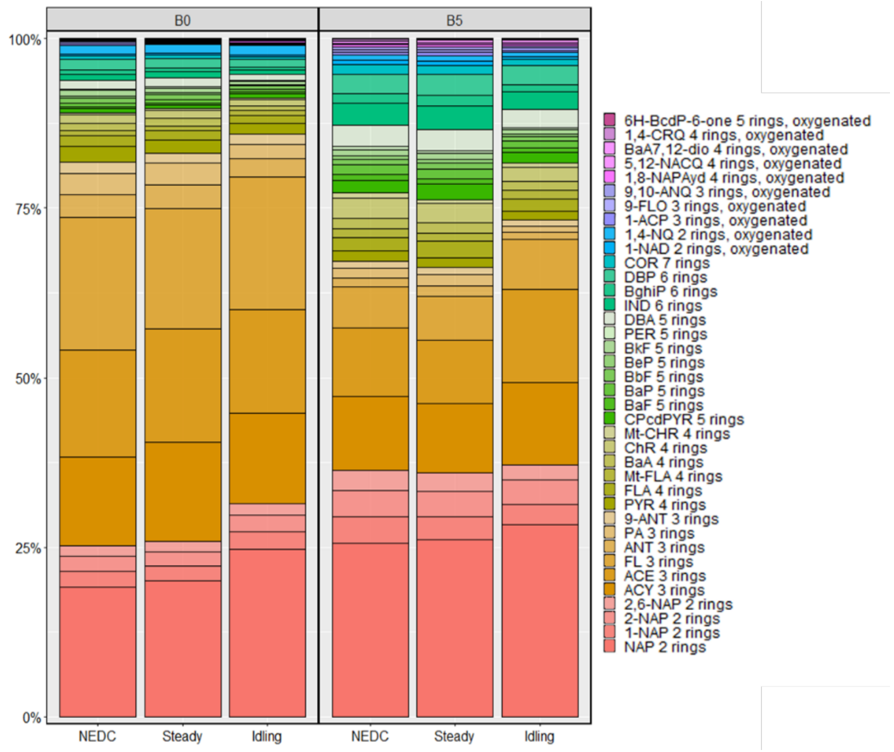

Figure 4: Composition of averaged fuel-based *EFs* (µg/kg) of PAHs and oxy-PAHs.

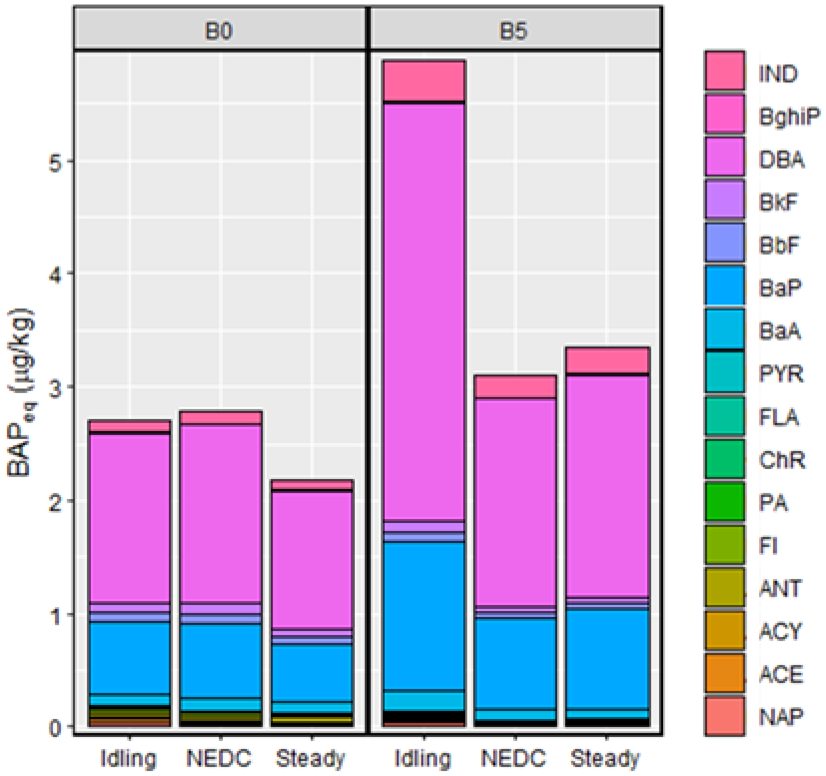

Figure 5: Composition of toxicity in terms of fuel-based *EFs* (µg/kg) of BAP$_{eq}$.